

Longitudinal-mode competition induced instabilities of Cr⁴⁺,Nd³⁺:Y₃Al₅O₁₂ self-Q-switched two-mode laser

Jun Dong and Ken-ichi Ueda

Citation: *Appl. Phys. Lett.* **87**, 151102 (2005); doi: 10.1063/1.2089153

View online: <http://dx.doi.org/10.1063/1.2089153>

View Table of Contents: <http://apl.aip.org/resource/1/APPLAB/v87/i15>

Published by the [American Institute of Physics](http://www.aip.org).

Additional information on *Appl. Phys. Lett.*

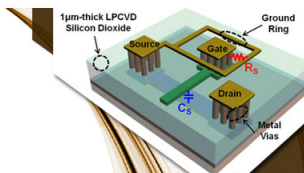
Journal Homepage: <http://apl.aip.org/>

Journal Information: http://apl.aip.org/about/about_the_journal

Top downloads: http://apl.aip.org/features/most_downloaded

Information for Authors: <http://apl.aip.org/authors>

ADVERTISEMENT

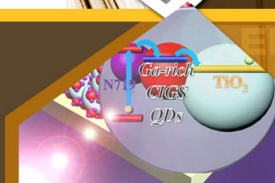


SURFACES AND INTERFACES

Focusing on physical, chemical, biological, structural, optical, magnetic and electrical properties of surfaces and interfaces, and more...

**EXPLORE WHAT'S
NEW IN APL**

SUBMIT YOUR PAPER NOW!



ENERGY CONVERSION AND STORAGE

Focusing on all aspects of static and dynamic energy conversion, energy storage, photovoltaics, solar fuels, batteries, capacitors, thermoelectrics, and more...

Longitudinal-mode competition induced instabilities of $\text{Cr}^{4+}, \text{Nd}^{3+}:\text{Y}_3\text{Al}_5\text{O}_{12}$ self- Q -switched two-mode laser

Jun Dong^{a)} and Ken-ichi Ueda

Institute for Laser Science, University of Electro-Communications, 1-5-1 Chofugaoka, Chofu, Tokyo 182-8585, Japan

(Received 25 May 2005; accepted 15 August 2005; published online 3 October 2005)

Stable single-longitudinal-mode laser pulses and instability of two-longitudinal-mode oscillation due to the spatial hole-burning effect were observed experimentally in a laser-diode pumped microchip $\text{Cr}^{4+}, \text{Nd}^{3+}:\text{Y}_3\text{Al}_5\text{O}_{12}$ self- Q -switched laser. We modified the multimode rate equations by including the spatial hole-burning effect in the active medium and the nonlinear absorption of the saturable absorber. The numerical simulations of the mode-competition dynamics of two-mode laser are in good agreement with the experimental data. Instability induced by the mode-competition dynamics was investigated by the evolution of the inversion population and the bleaching and recovery of the inversion population of the saturable absorber. © 2005 American Institute of Physics. [DOI: 10.1063/1.2089153]

Stable, high-beam-quality, passively Q -switched lasers with high peak power are good laser sources for light detecting and ranging, pollution monitoring, material processing, microsurgery, and so on. Passively Q -switched solid-state lasers are usually operated by using Nd^{3+} -doped materials as gain media and $\text{Cr}^{4+}:\text{Y}_3\text{Al}_5\text{O}_{12}$ [Cr^{4+} : yttrium–aluminum–garnet (YAG)] crystal as saturable absorber. Pulses with sub-nanosecond durations and several tens of kilowatt peak power have been achieved.¹ However, passively Q -switched pulses usually exhibit large jitters in peak power and in repetition rate that are undesirable for many applications. Pump-power-dependent pulse train bifurcation has been observed in a microchip laser;¹ however, the nonlinear dynamics of such bifurcation was not investigated in detail. Deterministic chaos of the fundamental mode oscillation² and the dynamics of transverse mode competition on the instabilities³ of passively Q -switched Nd:YAG laser with Cr^{4+} :YAG saturable absorber have been reported recently. Besides the nonlinear dynamics of the fundamental mode and the transverse modes, the longitudinal-mode competition also plays a very important role in the laser instabilities. Although continuous-wave microchip solid-state lasers are widely used to study the nonlinear effects such as chaos, antiphase dynamics and instabilities,^{4–8} there is no such report on the effects of longitudinal-mode competition on the instability of the microchip passively Q -switched laser with a saturable absorber. In this letter, we report experimental observations of instabilities in laser-diode-pumped $\text{Cr}^{4+}, \text{Nd}^{3+}:\text{Y}_3\text{Al}_5\text{O}_{12}$ (Cr,Nd:YAG) microchip self- Q -switched two-longitudinal-mode laser, and focus on the nonlinear dynamics of longitudinal-mode competition in the two-mode oscillation regime. Modified multimode rate equations are proposed including the cross-saturation effect due to the spatial hole-burning effect and the nonlinear absorption effect of the Cr^{4+} saturable absorber in the Cr,Nd:YAG crystal. Numerical solutions of the rate equations are obtained and the instability dynamics of Cr,Nd:YAG two-mode laser are reproduced.

The experiment was carried out with a plane-parallel, 1-mm-thick YAG crystal co-doped with 1 at. % Nd and 0.01 at. % Cr as gain medium. One surface of the crystal is coated for high transmission at 808 nm and total reflection at 1064 nm. The other surface is coated for anti-reflection at 1064 nm and total reflection at 808 nm. An output coupler with 15% transmission at 1064 nm was attached to the Cr,Nd:YAG crystal. A 1 W, continuous-wave, high-brightness 808 nm laser diode with a $50 \times 1 \mu\text{m}^2$ emission cross section was used as the pump source. Two lenses of 8 mm focal length were used to focus the pump beam on the crystal rear surface and to produce a pump light footprint in the crystal of about $75 \times 75 \mu\text{m}^2$. The laser was operated at room temperature. The Q -switched pulses were recorded by using a fiber-coupled InGaAs photodiode with a bandwidth of 16 GHz, and a 7 GHz Tektronix TDS7704B digital phosphor oscilloscope. The laser spectrum was analyzed by using an optical spectrum analyzer. The laser output beam profile was monitored using a charge coupled device camera both in the near field and the far field of the output coupler.

The average output power of the self- Q -switched laser as a function of the absorbed pump power is shown in Fig. 1. The absorbed pump power threshold was 60 mW, and stable single-longitudinal-mode oscillation was obtained when the absorbed pump power was kept below 170 mW. Above this

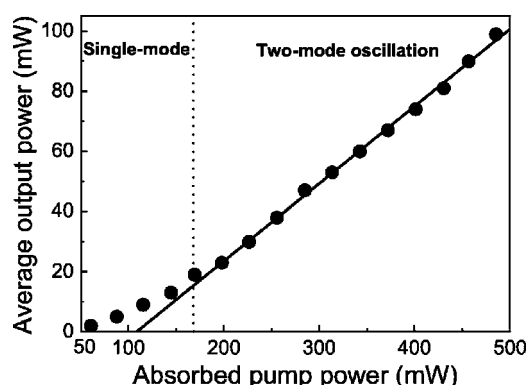


FIG. 1. The input-output power characteristics of a laser-diode-pumped microchip self- Q -switched laser.

^{a)} Author to whom correspondence should be addressed; electronic mail: dong@ils.uec.ac.jp

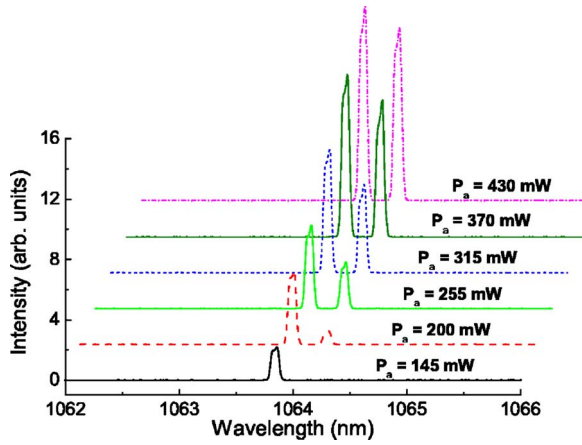


FIG. 2. (Color online) The evolution of the laser spectra around 1064 nm of self- Q -switched laser with the absorbed pump power. The spectral resolution is 0.01 nm.

value, the laser exhibited two-mode oscillations as shown in Fig. 2. Single-longitudinal-mode oscillation at 1063.86 nm was obtained. The main mode wavelength was 1063.88 nm, and secondary mode wavelength was 1064.19 nm for two-mode oscillation. The separation of two-mode oscillation under different pump power was about 0.31 nm; the linewidth of each mode was measured to be 0.06 nm. The optical slope efficiency was about 26%, and optical-to-optical efficiency was about 20.5%. A maximum average output power of 99 mW and the pulse energy of 2.8 μJ with pulse width (full width at half maximum) of 2.6 ns at repetition rate of 40 kHz were obtained when the absorbed pump power was 485 mW. A maximum peak power exceeding 1 kW was obtained. The output laser transverse intensity profile was close to fundamental transverse electromagnetic mode and was near-diffraction limited with M^2 of 1.2. It should be noted that stable single-longitudinal-mode oscillation could be obtained by increasing the pump beam spot incident on the laser crystal at higher pump power.

The instability dynamics of the self- Q -switched two-longitudinal-mode laser was studied experimentally by measuring the output pulse sequence intensity. Typical examples of the measured pulse trains of self- Q -switched single-longitudinal-mode and two-mode laser at different pump powers are shown in Fig. 3. The stable single-longitudinal-mode oscillation was observed and pulse repetition rate was

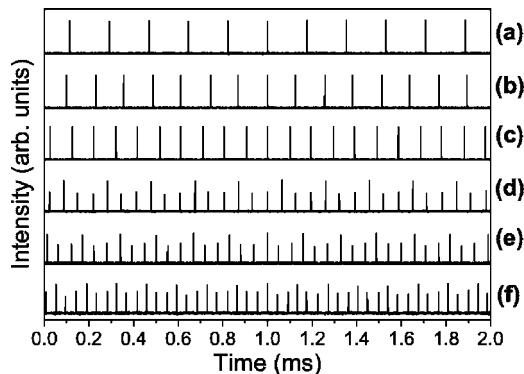


FIG. 3. The evolution of the output pulse sequences of self- Q -switched single-mode, and two-mode oscillation with the absorbed pump power, (a) $P_a=85$ mW, (b) $P_a=115$ mW, (c) $P_a=145$ mW for the single-mode oscillation, (d) $P_a=200$ mW, (e) $P_a=255$ mW, (f) $P_a=315$ mW for the two-mode oscillation which show the pulse instability.

found to increase with the absorbed pump power, as shown in Figs. 3(a)–3(c). When the laser was working in two-mode regime, the output pulse train was characterized by a modulation of the pulse intensity with a period three times that of the repetition period, as shown in Figs. 3(d)–3(f). The most interesting thing is that the pulsations occurred for the first mode with the highest gain characterized by two pulses with nearly equal intensities, the secondary mode with higher pulse intensity appears alternatively with two pulses of the first mode. There is repetition rate jitter for the first mode pulses and secondary mode pulse. The output pulsation characteristics of this two-mode oscillation of microchip Cr,Nd:YAG laser is caused by the cross-saturation mechanism due to the spatial hole burning coupling the modes via population gratings and the nonlinear absorption of the Cr^{4+} saturable absorber, but it is different from the antiphase states observed in Ref. 8. With further increase of the pump power, the pulsation characteristics of the output laser do not change, only the time interval between each pulse is shortened as shown in Figs. 3(d)–3(f).

To better understand the unstable nature of the two-longitudinal-mode self- Q -switched microchip laser, we modified the multimode laser rate equations by taking into account the cross-saturation dynamics that is due to the spatial hole-burning effect and the nonlinear absorption of the saturable absorber⁹ as follows:

$$\frac{dn_0}{dt} = w - n_0 - \sum_{i=1}^N \gamma_i \left(n_0 - \frac{n_i}{2} \right) \phi_i, \quad (1)$$

$$\frac{dn_i}{dt} = \gamma_i n_0 \phi_i - n_i \left(1 + \sum_{i=1}^N \gamma_i \phi_i \right), \quad (2)$$

$$\frac{d\phi_i}{dt} = K \left[\left(\gamma_i \left(n_0 - \frac{n_i}{2} \right) - 1 - 2(\delta_1 N_g - \delta_2 (N_0 - N_g)) l \right) \phi_i + \varepsilon n_0 \right], \quad (3)$$

$$\frac{dN_g}{dt} = (N_0 - N_g) \xi - \delta_1 N_g \sum_{i=1}^N \phi_i \quad (4)$$

with $i=1, \dots, N$. In Eqs. (1)–(4), time is normalized to the fluorescence lifetime τ of the gain medium; w is the relative pump rate normalized to the first-lasing-mode absorbed pump power threshold; n_0 and n_i are the space-averaged population inversion density and the normalized Fourier components of the population inversion density for the i th mode normalized to the first-lasing-mode threshold population inversion density; ϕ_i is the normalized photon density, $\gamma_i \leq 1$ is the relative gain with respect to the first lasing mode, $K = \tau / \tau_c$ is the lifetime ratio of the fluorescence lifetime of the gain medium to the photon lifetime inside the laser cavity, l is the length of the saturable absorber, ε is the spontaneous emission coefficient, δ_1 and δ_2 are the ratio of the ground state absorption cross section and the excited state absorption cross section of Cr^{4+} saturable absorber to the stimulated emission cross section of the gain medium of Nd^{3+} , respectively. N_g, N_0 are the population inversion density and the total population density of Cr^{4+} saturable absorber normalized to the first-lasing-mode threshold. ξ is the

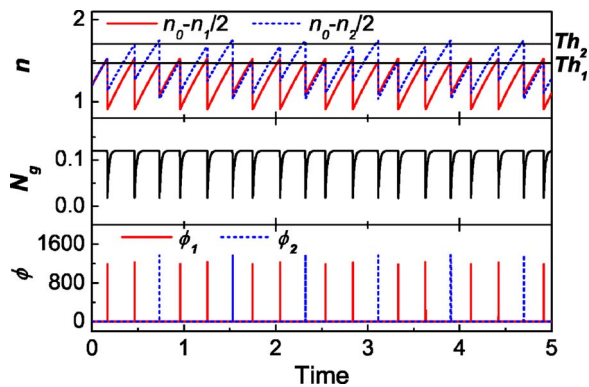


FIG. 4. (Color online) Numerical simulation of the pulse sequences of the population inversion of each mode, the population inversion of the saturable absorber and the photon intensities for two-mode instability oscillation when the pump power ratio w is 3.3. Other parameters (see Ref. 10) used are $K=1.5 \times 10^7$, $\delta_1=20.1$, $\delta_2=3.6$, $\xi=61.8$, $\varepsilon=1.2 \times 10^{-7}$, $\tau=210 \mu\text{s}$, $\gamma_1=1$, $\gamma_2=0.8$. Th_1 and Th_2 are the threshold for the first mode and secondary mode, respectively.

ratio of the fluorescence lifetime of gain medium to the lifetime of the saturable absorber.

Based on the parameters of our Cr,Nd:YAG laser, we numerically solved the rate equations by using the fourth-order Runge–Kutta method. A typical numerical solution of the population inversion density of two modes, $n_0 - n_1/2$, $n_0 - n_2/2$, the population inversion density of the saturable absorber, N_g , and the photon density for two-mode oscillation, ϕ_1 , ϕ_2 is shown in Fig. 4. These numerical solutions of pulse repetition rate and average pulse width for two-mode oscillation reproduced the experimental results shown in Fig. 3(d). The numerically calculated pulse trains clearly show that not only the pulse amplitudes but also their pulse intervals vary periodically. A smaller pulse interval follows a larger pulse, suggesting that the pulse repetition rate jitter is also an intrinsic property of the laser system. The unstable behavior of the alternative three-pulse oscillation of Cr,Nd:YAG self- Q -switched laser under continuous-wave pumping can be explained from Fig. 4 as follows. The time interval between the pulses is mainly governed by the buildup time of the population inversion n to reach the threshold value, and also by the buildup time of the photon density ϕ , which is very short compared to the buildup time of the population inversion, after n exceeds the threshold. Under continuous-wave pumping, the first mode of highest gain will reach its threshold first while the second mode is suppressed. Therefore, the decrease of the population inversion $n_0 - n_1/2$ of the first mode, just after the oscillation, is more significant than that of $n_0 - n_2/2$ for the second mode. Because the threshold for the second mode is higher than that for first mode ($\text{Th}_2 > \text{Th}_1$), the inversion population for the first mode still reaches its threshold faster than that for the second mode; the second pulse of the first mode will oscillate and suppress the oscillation for the second mode. So

the two-pulse oscillation for the first mode was developed. After the pulse development for the first mode, the population inversion for the first mode was depleted dramatically comparing to the second mode. Then, the recovery time of the population inversion to its threshold value is shorter for the second mode than for the first mode, and the second mode oscillation suppresses the first mode. This kind of laser pulse train of two-mode oscillates periodically under the continuous-wave pumping and the nonlinear absorption of the saturable absorber, the delay time of each mode being determined by the nonlinear absorption of the saturable absorber and the threshold for each mode. Similar pulsation behaviors of two-mode oscillation have been obtained generally for appropriate parameter w from 2.5 to 8. The pulsation instability dynamics of two-mode oscillation does not change with the increase of the pump power, however, the time interval between the pulses will be shortened with the pump power. The good agreement between the numerical calculation and the experimental results of the instability and the repetition rate jitter for two-longitudinal-mode oscillation shows that the instability of the two-mode oscillation is an intrinsic property of such laser, which is due to the spatial hole burning of the gain medium and the nonlinear absorption of the saturable absorber.

In conclusion, the instability and the repetition rate jitter were observed in a laser-diode-pumped Cr,Nd:YAG microchip self- Q -switched two-mode laser. The instability and the jitter of this laser were caused by the longitudinal-mode competition. The numerical simulations based on the multi-mode passively Q -switched laser rate equations almost reproduce the observed instability dynamics of the two-mode oscillation and confirm that the unstable dynamics of Cr,Nd:YAG self- Q -switched laser is an intrinsic property of such laser. The stable single-longitudinal-mode laser pulse in compact microchip Cr,Nd:YAG self- Q -switched laser can be achieved by using suitable pump beam diameter.

This work was supported by the 21st Century Center of Excellence (COE) program of the Ministry of Education, Science and Culture of Japan. The authors thank J. F. Bisson for his reading of the manuscript.

¹J. J. Zayhowski and C. Dill III, *Opt. Lett.* **19**, 1427 (1994).

²D. Y. Tang, S. P. Ng, L. J. Qin, and X. L. Meng, *Opt. Lett.* **28**, 325 (2003).

³M. Wei, C. Chen, and K. Tu, *Opt. Express* **12**, 3972 (2004).

⁴K. Otsuka, Y. Asakawa, R. Kawai, S. Hwong, and J. Chern, *Jpn. J. Appl. Phys., Part 2* **37**, L1523 (1998).

⁵K. Otsuka, S. Hwong, and B. Nguyen, *Phys. Rev. A* **61**, 053815 (2000).

⁶K. Otsuka, J. Ko, T. Kubota, S. Hwong, T. Lim, J. Chern, B. Nguyen, and P. Mandel, *Opt. Lett.* **26**, 1060 (2001).

⁷K. Otsuka, *Phys. Rev. Lett.* **67**, 1090 (1991).

⁸M. A. Larotonda, A. M. Yacomotti, and O. E. Martinez, *Opt. Commun.* **169**, 149 (1999).

⁹C. L. Tang, H. Statz, and G. Demars, *J. Appl. Phys.* **34**, 2289 (1963).

¹⁰J. Dong and P. Deng, *Opt. Commun.* **220**, 425 (2003).